

On the connection between the self-sputter yield and deposition rate in HiPIMS operation

J. T. Guðmundsson^{1,2}, M. Rudolph³, K. Barynova¹,
J. Fischer⁴, S. Suresh Babu¹, N. Brenning^{2,4}, M. A. Raadu²,
and D. Lundin⁴

¹ Science Institute, University of Iceland, Reykjavik, Iceland

² KTH Royal Institute of Technology, Stockholm, Sweden

³ Leibniz Institute of Surface Engineering (IOM), Leipzig, Germany

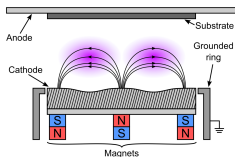
⁴ Plasma and Coatings Physics, Linköping University, Sweden

19th International Conference on Plasma Surface Engineering,
Erfurt, Germany

September 2, 2024



Introduction – Magnetron sputtering



Gudmundsson and Lundin (2020) in High Power Impulse Magnetron Sputtering Discharge, Elsevier, 2020

- Magnetron sputtering has been a highly successful technique that is essential in a number of industrial applications
- In a high power impulse magnetron sputtering (HiPIMS) the discharge is driven by high power pulses of low repetition frequency, and with low duty cycle
- This results in high discharge current density, increased electron density, and increased ionization of the sputtered species

Gudmundsson (2020) PSST **29** 113001

Overview

- Thin film deposition
- The ionization region model (IRM)
- Deposition rate vs ionized flux fraction
- Working gas rarefaction
- Summary

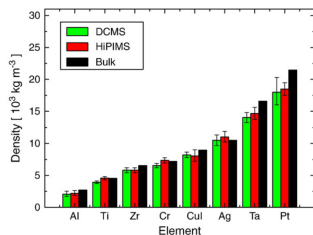


Thin film deposition



Thin film deposition

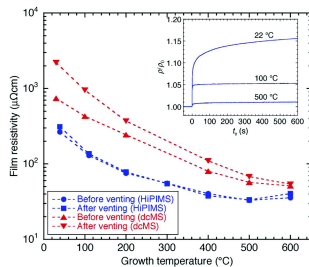
- The film mass density is always higher
- The surfaces are significantly smoother – when depositing with HiPIMS compared to dcMS at the same average power
- The films typically exhibit better crystallinity, and overall improved film properties
 - lower electrical resistivity
 - improved optical properties
 - improved mechanical properties
 - better oxidation resistance



From Samuelsson et al. (2010) SCT **202** 591

Thin film deposition

- TiN as diffusion barriers for interconnects
- HiPIMS deposited films have significantly lower resistivity than dcMS deposited films on SiO₂ at all growth temperatures due to reduced grain boundary scattering
- Thus, ultrathin continuous TiN films with superior electrical characteristics and high resistance towards oxidation can be obtained with HiPIMS at reduced temperatures

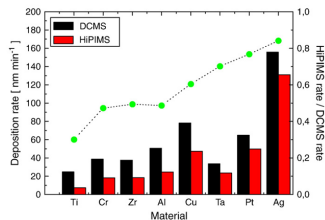


From Magnus et al. (2012) IEEE EDL **33** 1045



Thin film deposition

- There is a drawback
- The deposition rate is lower for HiPIMS when compared to dcMS operated at the same average power
- The HiPIMS deposition rates are typically in the range of 30 – 85% of the dcMS rates depending on target material
- Many of the ions of the target material are attracted back to the target surface by the cathode potential



From Samuelsson et al. (2010) SCT **202** 591

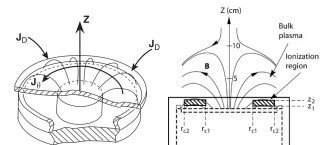
The ionization region model (IRM)



Ionization region model

- The ionization region model (IRM) is a time-dependent volume averaged plasma chemical model of the ionization region (IR) of the HiPIMS discharge
- The IRM gives the temporal evolution of the densities of ions, neutrals and electrons
- The IRM gives also two internal parameters that are of importance
 - α_t – ionization probability
 - β_t – back-attraction probability

Detailed model description is given in Huo et al. (2017) JPD **50** 354003



The definition of the volume covered by the IRM

- The IR is defined as an annular cylinder of width $w_{rt} = r_{c2} - r_{c1}$ and thickness $L = z_2 - z_1$, extends from z_1 to z_2 axially away from the target



Ionization region model

- The temporal development is defined by a set of ordinary differential equations giving the first time derivatives of
 - the electron energy
 - the particle densities for all the particles (except electrons)
- The species assumed in the non-reactive-IRM are
 - cold electrons e^C , hot electrons e^H
 - argon atoms $Ar(3s^23p^6)$, warm argon atoms in the ground state Ar^W , hot argon atoms in the ground state Ar^H , Ar^m ($1s_5$ and $1s_3$) (11.6 eV), argon ions Ar^+ (15.76 eV), doubly ionized argon ions Ar^{2+} (27.63 eV)
 - Metal atoms, sometimes metastable states, metal ion M^+ , and doubly ionized metal ions M^{2+}

Detailed model description is given in Huo et al. (2017), JPD **50** 354003



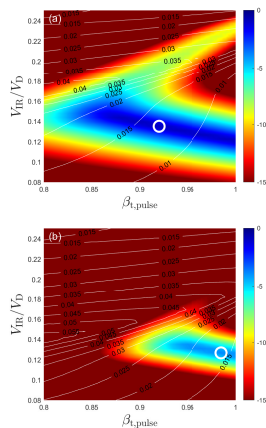
Ionization region model

- As an example the particle balance equation for the metal ion M^+ is

$$\begin{aligned}
 \frac{dn_{M^+}}{dt} = & \underbrace{k_{iz,M}^c n_e n_M + k_{iz,M}^h n_e n_M}_{\text{electron impact ionization}} + \underbrace{k_{P,iz} n_{Ar^m} n_M}_{\text{Penning ionization}} \\
 & + \underbrace{k_{chexc,1} n_M n_{Ar^+} + k_{chexc,2} n_{M^{2+}} n_{Ar}}_{\text{charge exchange}} - \underbrace{k_{iz,M^+}^c n_e n_{M^+} - k_{iz,M^+}^h n_e n_{M^+}}_{\text{electron impact ionization to create } M^{2+}} \\
 & - \underbrace{\frac{\Gamma_{M^+}^{RT} + \Gamma_{M^+}^{BP} (S_{IR} - S_{RT})}{V_{IR}}}_{\text{ion flux out of the ionization region}}
 \end{aligned}$$

Ionization region model

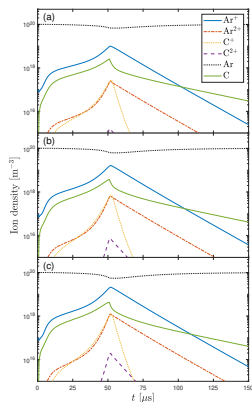
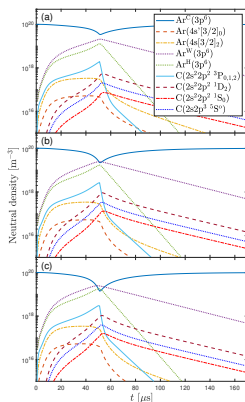
- The IRM is a semi-empirical discharge model and requires the measured discharge current and voltage waveforms
- The IRM has three unknown fitting parameters
 - the ion back-attraction probability for the metal ions $\beta_{t,pulse}$ and gas ions $\beta_{g,pulse}$
 - the potential drop across the IR $f = V_{IR}/V_D$
 - the electron recapture probability $r = 0.7$
- This leaves the $(\beta_{t,pulse}, f)$ parameter space to be explored through the model fitting procedure – the blue zones in the fitting map indicate the smallest mean square error



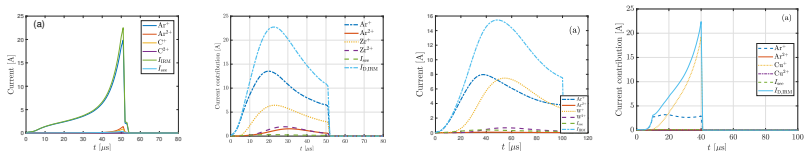
Ionization region model

- The temporal evolution of the neutral and ion densities in a discharge with graphite target
- Ar^+ ions dominate the discharge – constitute over 90% of the discharge current
- Working gas rarefaction is apparent
- The back-attraction probability is high

$$\beta_{t,\text{pulse}} > 0.83$$



Ionization region model



C: PSST (2021) **30** 115017 Zr: JVSTA (2024) **42** 043007 W: PSST (2022) **31** 065009 Cu: SCT (2022) **442** 128189

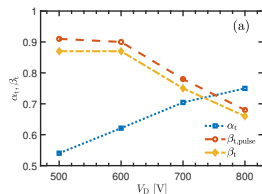
- The temporal evolution of the discharge current composition at the target surface for three different targets
- With Cu target Cu⁺ ions dominate, with graphite target Ar⁺ ions dominate
- For Zr and W targets there is a mix of Ar⁺ and metal ions

Ionization region model

- For tungsten target the ionization probability α_t increases with increased discharge voltage
- The peak discharge current increases with increased discharge voltage
- Earlier we have argued that the ionization probability depends only on the peak discharge current and increases with increased peak discharge current

Rudolph et al. (2022) JPD **55** 015202

- The back-attraction probability $\beta_{t,pulse}$ decreases with increased discharge voltage



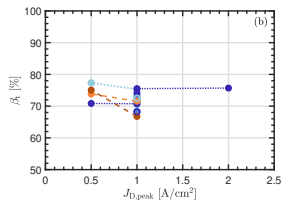
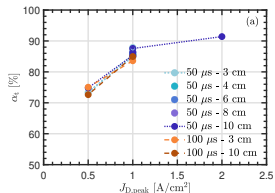
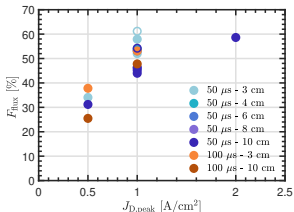
A discharge with a tungsten target

From Suresh Babu et al. (2022) PSST **31** 065009



Ionization region model

- For zirconium target the ionization probability α_t increases with increased current density
- The back-attraction probability $\beta_{t,pulse}$ does not show any trend



- The measured ionized flux fraction is used to lock the model

discharge with a zirconium target

Deposition rate vs ionized flux fraction



Deposition rate – α_t and β_t

- We can relate the measured quantities normalized deposition rate $F_{\text{DR,sput}}$ and the ionized flux fraction $F_{\text{ti,flux}}$

$$F_{\text{DR,sput}} = \frac{\Gamma_{\text{DR}}}{\Gamma_0} = (1 - \alpha_t \beta_t)$$

$$F_{\text{ti,flux}} = \frac{\Gamma_{\text{DR,ions}}}{\Gamma_{\text{DR,sput}}} = \frac{\Gamma_0 \alpha_t (1 - \beta_t)}{\Gamma_0 (1 - \alpha_t \beta_t)} = \frac{\alpha_t (1 - \beta_t)}{(1 - \alpha_t \beta_t)}$$

to the internal parameters back attraction probability β_t

$$\beta_t = \frac{1 - F_{\text{DR,sput}}}{1 - F_{\text{DR,sput}}(1 - F_{\text{ti,flux}})}$$

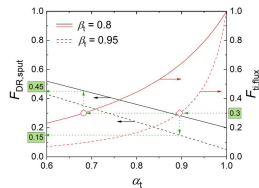
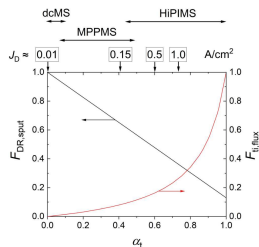
and ionization probability α_t

$$\alpha_t = 1 - F_{\text{DR,sput}}(1 - F_{\text{ti,flux}})$$



Deposition rate – Optimization

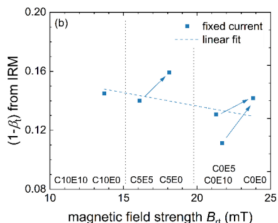
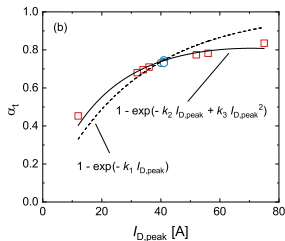
- There are two measures of how good a HiPIMS discharge is:
 - the fraction $F_{DR,sput}$ of all the sputtered material that reaches the diffusion region (DR)
 - the fraction $F_{ti,flux}$ of ionized species in that flux
- There is a trade off between the goals of higher $F_{DR,sput}$ and higher $F_{ti,flux}$
- The question that remains:
 - How can we vary the ionization probability α_t and maybe more importantly the back-attraction probability β_t ?



Deposition rate – Optimization

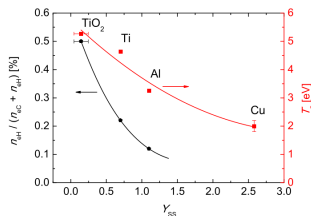
- The internal discharge parameters α_t and β_t from the ionization region model (IRM)
- The ionization probability α_t increases with increased discharge current
- The ion escape fraction $(1 - \beta_t)$ versus the magnetic field strength

From Rudolph et al. (2022) JPD **55** 015202



Deposition rate – Optimization

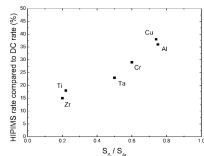
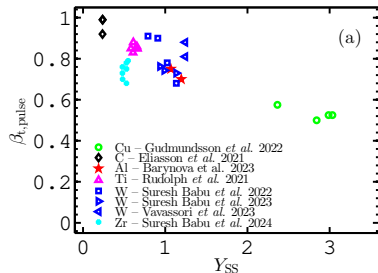
- We know that the electron temperature and the hot electron density fall with increased sputter yield
- Held *et al.* observed that titanium atoms are ionized within 0.5 mm from the target surface (high $\beta_{t,pulse}$), while aluminum and chromium atoms can travel further before being ionized (lower $\beta_{t,pulse}$)
- The measured electron temperature is 4.5 eV for titanium target compared to 2.6 eV (aluminum) and 1.5 eV (chromium)



From Brenning et al. (2017) PSST **26** 125003

Deposition rate – Optimization

- What determines the back-attraction probability ?
- How can one influence the back-attraction probability ?
- The back-attraction probability $\beta_{t,pulse}$, determined by IRM, versus the self-sputter yield for various target materials
- The data indicate that the back-attraction probability decreases roughly linearly with increased self-sputter yield

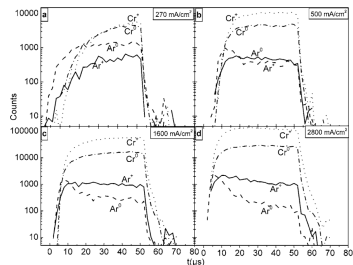


Working gas rarefaction



Working gas rarefaction

- The sputtered species enter the discharge at considerable energy, which is determined by the cohesive energy of the solid target
- The interaction between the energetic sputtered particles and the working gas atoms can lead to a reduction in the working gas density – as has been observed experimentally in the HiPIMS discharge
- Working gas rarefaction has been observed in the HiPIMS discharge



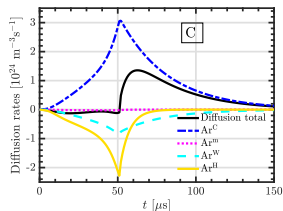
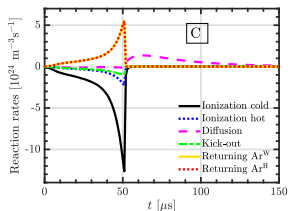
From Alami et al. (2006) APL **89**(15) 154104

Working gas rarefaction

- HiPIMS discharge with graphite target and $J_{D,peak} = 1 \text{ A cm}^{-2}$

Eliasson et al. (2021) PSST **30** 115017

- Argon atoms are lost mainly through electron impact ionization by primary and secondary electrons
- Contributions of kick-out and charge-exchange are negligible
- Diffusion contributes to a net loss of argon atoms during the pulse, but to a flow into the ionization region after the pulse is off

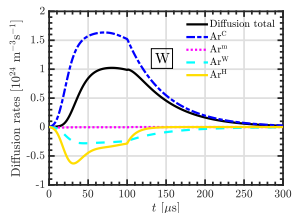
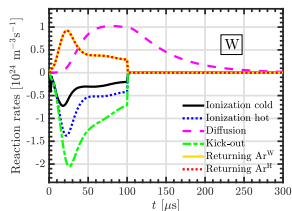


Working gas rarefaction

- HiPIMS discharge with tungsten target and $J_{D,peak} = 0.54 \text{ A cm}^{-3}$

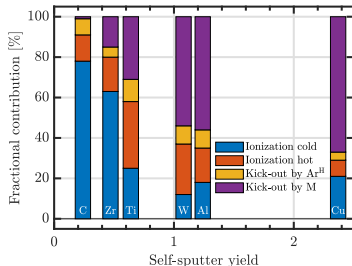
Suresh Babu et al. (2022) PSST **31** 065009

- The main contributor to the loss of argon atoms from the IR is kick-out by tungsten atoms sputtered from the target (39 – 48 % contribution)
- The second most important loss process is electron impact ionization by secondary electrons followed by electron impact ionization by the primary electrons



Working gas rarefaction

- The relative contributions of the various processes to working gas rarefaction varies greatly depending on the target material
- The various contributions versus the atomic mass of the target material for $J_{D,peak} \sim 1 \text{ A/cm}^2$ and $p_g \sim 1 \text{ Pa}$



From Barynova et al. PSST **33**(6) 065010



Summary



Summary

- The discharge current composition at the target surface depends on the target material
- There is an inescapable conflict between the goals of higher deposition rate and higher fraction of ionized species in the sputtered material flux
- The back-attraction probability appears to depend on the self-sputter yield – it is lower for higher self-sputter yield
- The main contributor to working gas rarefaction for low sputter yield target is electron impact ionization, while for targets with high sputter yield kick-out by the sputtered species is the main contributor



Thank you for your attention

tumi@hi.is

The slides can be downloaded at

<http://langmuir.raunvis.hi.is/~tumi/ranns.html>



Further reading

- J. T. Gudmundsson, Physics and technology of magnetron sputtering discharges, Plasma Sources Science and Technology, **29**(11) (2020) 113001
- J. T. Gudmundsson, André Anders, and Achim von Keudell, Foundations of physical vapor deposition with plasma assistance, Plasma Sources Science and Technology, **31**(8) (2022) 083001
- Daniel Lundin, Tiberiu Minea and Jon Tomas Gudmundsson (eds.), High Power Impulse Magnetron Sputtering: Fundamentals, Technologies, Challenges and Applications, Elsevier, 2020



References

- Alami, J., K. Sarakinos, G. Mark, and M. Wuttig (2006). On the deposition rate in a high power pulsed magnetron sputtering discharge. *Applied Physics Letters* 89(15), 154104.
- Barynova, K., S. Suresh Babu, M. Rudolph, J. Fischer, D. Lundin, M. A. Raadu, N. Brenning, and J. T. Gudmundsson (2024). On working gas rarefaction in high power impulse magnetron sputtering. *Plasma Sources Science and Technology* 33(6), 065010.
- Brenning, N., A. Butler, H. Hajihoseini, M. Rudolph, M. A. Raadu, J. T. Gudmundsson, T. Minea, and D. Lundin (2020). Optimization of HiPIMS discharges: The selection of pulse power, pulse length, gas pressure, and magnetic field strength. *Journal of Vacuum Science and Technology A* 38(3), 033008.
- Brenning, N., J. T. Gudmundsson, M. A. Raadu, T. J. Petty, T. Minea, and D. Lundin (2017). A unified treatment of self-sputtering, process gas recycling, and runaway for high power impulse sputtering magnetrons. *Plasma Sources Science and Technology* 26(12), 125003.
- Eliasson, H., M. Rudolph, N. Brenning, H. Hajihoseini, M. Zanáška, M. J. Adriaans, M. A. Raadu, T. M. Minea, J. T. Gudmundsson, and D. Lundin (2021). Modeling of high power impulse magnetron sputtering discharges with graphite target. *Plasma Sources Science and Technology* 30(11), 115017.
- Gudmundsson, J. T. (2020). Physics and technology of magnetron sputtering discharges. *Plasma Sources Science and Technology* 29(11), 113001.
- Gudmundsson, J. T., N. Brenning, D. Lundin, and U. Helmersson (2012). The high power impulse magnetron sputtering discharge. *Journal of Vacuum Science and Technology A* 30(3), 030801.
- Gudmundsson, J. T. and D. Lundin (2020). Introduction to magnetron sputtering. In D. Lundin, T. Minea, and J. T. Gudmundsson (Eds.), *High Power Impulse Magnetron Sputtering: Fundamentals, Technologies, Challenges and Applications*, pp. 1–48. Amsterdam, The Netherlands: Elsevier.
- Hajihoseini, H., M. Čada, Z. Hubička, S. Ůnaldi, M. A. Raadu, N. Brenning, J. T. Gudmundsson, and D. Lundin (2019). The effect of magnetic field strength and geometry on the deposition rate and ionized flux fraction in the HiPIMS discharge. *Plasma* 2(2), 201–221.
- Held, J., V. Schulz-von der Gathen, and A. von Keudell (2023). Ionization of sputtered material in high power impulse magnetron sputtering plasmas – comparison of titanium, chromium and aluminum. *Plasma Sources Science and Technology* 32(6), 065006.

References

- Helmersson, U., M. Lattemann, J. Alami, J. Bohlmark, A. P. Ehasarian, and J. T. Gudmundsson (2005). High power impulse magnetron sputtering discharges and thin film growth: A brief review. In *Proceedings of the 48th Society of Vacuum Coaters Annual Technical Conference*, pp. 458 – 464.
- Huo, C., D. Lundin, J. T. Gudmundsson, M. A. Raadu, J. W. Bradley, and N. Brenning (2017). Particle-balance models for pulsed sputtering magnetrons. *Journal of Physics D: Applied Physics* 50(35), 354003.
- Magnus, F., A. S. Ingason, S. Olafsson, and J. T. Gudmundsson (2012). Nucleation and resistivity of ultrathin TiN films grown by high power impulse magnetron sputtering. *IEEE Electron Device Letters* 33(7), 1045 – 1047.
- Raadu, M. A., I. Axnäs, J. T. Gudmundsson, C. Huo, and N. Brenning (2011). An ionization region model for high power impulse magnetron sputtering discharges. *Plasma Sources Science and Technology* 20(6), 065007.
- Rudolph, M., N. Brenning, H. Hajihoseini, M. A. Raadu, T. M. Minea, A. Anders, D. Lundin, and J. T. Gudmundsson (2022). Influence of the magnetic field on the discharge physics of a high power impulse magnetron sputtering discharge. *Journal of Physics D: Applied Physics* 55(1), 015202.
- Rudolph, M., H. Hajihoseini, M. A. Raadu, J. T. Gudmundsson, N. Brenning, T. M. Minea, A. Anders, and D. Lundin (2021). On how to measure the probabilities of target atom ionization and target ion back-attraction in high-power impulse magnetron sputtering. *Journal of Applied Physics* 129(3), 033303.
- Samuelsson, M., D. Lundin, J. Jensen, M. A. Raadu, J. T. Gudmundsson, and U. Helmersson (2010). On the film density using high power impulse magnetron sputtering. *Surface and Coatings Technology* 202(2), 591–596.
- Suresh Babu, S., M. Rudolph, D. Lundin, T. Shimizu, J. Fischer, M. A. Raadu, N. Brenning, and J. T. Gudmundsson (2022). Ionization region model of a high power impulse magnetron sputtering of tungsten. *Plasma Sources Science and Technology* 31(6), 065009.
- Suresh Babu, S., J. Fischer, M. Rudolph, D. Lundin, and J. T. Gudmundsson (2024). Modeling of high power impulse magnetron sputtering discharges with a zirconium target. *Journal of Vacuum Science and Technology A* 42(4), 043007.

